IEEE Access
Multidisciplinary | Rapid Review | Open Access Journal

Received July 4, 2020, accepted July 20, 2020, date of publication July 29, 2020, date of current version August 12, 2020.

Digital Object Identifier 10.1109/ACCESS.2020.3012686

Enhanced Fractional Chaotic Whale Optimization Algorithm for Parameter Identification of Isolated Wind-Diesel Power Systems

YASHAR MOUSAVI[1], (Student Member, IEEE), ALIREZA ALFI[2], (Senior Member, IEEE), AND IBRAHIM BEKLAN KUCUKDEMIRAL[1], (Senior Member, IEEE)

[1]Department of Applied Science, School of Computing, Engineering and Built Environment, Glasgow Caledonian University, Glasgow G4 0BA, U.K.
[2]Faculty of Electrical and Robotic Engineering, Shahrood University of Technology, Shahrood 36199-95161, Iran

Corresponding author: Alireza Alfi (a_alfi@shahroodut.ac.ir)

ABSTRACT Parameters identification of isolated wind-diesel power systems (WDPS) is a significant issue in stability analysis of the power system as well as guaranteeing the power generation through the control system. In this article, enhanced whale optimization algorithms (EWOA) are proposed to deal with the parameter identification problem of a WDPS system. The proposed EWOA effectively tackles the premature convergence problem of WOA by splitting the population into two subpopulations and updating the position of each whale according to the position of the best agent in its current subpopulation, the position of the other subpopulation's best agent, and the position of the best neighboring agent. Furthermore, fractional chaotic maps are embedded in the search process of EWOA to increase its performance in terms of accuracy. For validation purposes, the proposed algorithms are applied to identify the unknown parameters of WDPS, where different statistical analyzes and comparisons are carried out with other recent state-of-the-art algorithms. Simulation results confirm that the algorithms have less deviation in parameter estimation, more convergence speed, and higher precision in comparison with other algorithms.

INDEX TERMS Optimization, parameter identification, whale optimization algorithm, wind-diesel power system.

I. INTRODUCTION

Renewable energy systems have received extensive attention during the past few decades due to their extensive positive effects on air pollution through decreasing greenhouse-gas emissions to the atmosphere [1]–[3]. With the daily growth of technology throughout the world, the demand for constant and reliable power is increasing significantly. Among all renewable energy resources, wind power generation technology has become the leading power supplying system to deal with this surging power demand [4]–[7]. Isolated wind-diesel power systems (WDPSs) are practical solutions to supply power for the remote facilities, islands, and rural communities where their connection to the central energy supply system is disconnected or somehow limited [6].

Isolated wind-diesel power systems consist of many parts consisting of semiconductors, electronic components, and mechanical gears, which are all inevitably prone to changes in their characteristic variations due to aging and faults. This may lead to reduction in efficiency of the system over time. Since the isolated WDPS has contributed a small yet critical portion of the world's power production, it is vital to guarantee the power generation through reliable and authentic control strategies [8]. To provide an accurate control system, it is crucial to describe the exact behaviour of the WDPS under operation using an accurate model. The model must closely represent the behaviour of the system, while the accuracy of the model mainly depends on its parameters. Low precision of the system parameters will cause significant error and failure in the control system [9]. Hence, precise parameter identification of the system is a necessity. However, it has found to be a complicated and challenging task due to the highly nonlinear structure of the system.

The parameter identification can be considered as an optimization problem having an appropriate criterion, which is a function of estimation error of the system parameters.

The associate editor coordinating the review of this manuscript and approving it for publication was Diego Oliva.

Various optimization techniques have been utilized to handle this problem. Traditional optimization methods, such as Gradient Descent [10] and Newton Raphson [11], seem to be inefficient due to their dependency on initial conditions and differentiating the objective function. Alternatively, meta-heuristic methods have been proven to be practical approaches to deal with different parameter identification problems [12]–[25] as well as practical optimization problems [25]–[28]. A parameter estimation strategy using whale optimization algorithm (WOA) was investigated to develop a precise fuel cell model [12]. A modified bacterial foraging algorithm was also investigated to identify the parameters of fractional-order systems [13]. Aiming at enhancing the exploration and exploitation performances of the basic gravitational search algorithms (GSA), improved GSAs were proposed in [14], [15] for precisely identifying the parameter of water turbine regulation systems. Improved ant lion optimization algorithm augmented with particle swarm optimization [17], and modified GSA [18] were also proposed for parameter identification of hydraulic turbine governing systems. Various optimization algorithms have been introduced and implemented to identify the photovoltaic (PV) parameters [19]–[24]. To name a few, modified cat swarm optimization algorithm [22], improved JAYA optimization algorithm [23], and flexible particle swarm optimization algorithm with an elimination phase [20] for parameters estimation of one-diode and two-diode PV models, as well as sunflower optimization for three-diode PV model [24]. Considering the aforementioned literature, the significant performance of optimization algorithms in parameter identification of industrial systems is apparent, which has attracted an emerging interest among researchers to develop and investigate more efficient methodologies.

The whale optimization algorithm as one of the most recent evolutionary algorithms motivated by the hunting behaviour of humpback whales [29], has been utilized for distinct optimization problems in recent years [30], [31]. The spiralling mechanism represents the exploitation phase consisting of encircling the prey and the spiral bubble-net feeding manoeuvre; while, the exploration phase is carried out by a random search for prey. Although WOA is proven to yield superior performance over many optimization algorithms in terms of solving complex optimization problems [32], [33], it still suffers from premature convergence when it comes to solving large-scale problems, which defects its performance. Consequently, various modifications have been reported in the literature to enhance its exploration and exploitation capabilities and achieve better performance. Authors in [34] developed the WOA based on Pareto dominance to solve multiobjective optimization problems. This algorithm used an exterior archive as a storage for the non-dominated solutions detected during the optimization mechanism. Taking advantage of a cosine function-based nonlinear dynamic strategy, a modified WOA was proposed in [35] to equilibrate the exploitation and exploration abilities to enhance the algorithm's efficiency for solving large-scale optimization problems. In [36], a refraction-learning-based WOA augmented with a modified Logistic-model-based conversion parameter update rule was developed to make a trade-off between diversity and convergence during the search process of WOA when solving high-dimensional problems. In this context, in order to solve the premature convergence of WOA and modify the exploration process, an enhanced WOA based on quadratic interpolation was proposed [37]. In addition, modified versions of WOA have achieved remarkable results in other applications, such as water resources demand estimation [38], maximizing the power capture of variable-speed wind turbines [39], task allocation [40], parameter identification of solar cell diode model [41], quadratic assignment problem [42], terminal voltage control of fuel cells [43], and short-term natural gas consumption prediction [44]. Although these modifications have yielded some performance enhancements to the conventional WOA, they still suffer from other drawbacks such as lack of exploitation accuracy [36]–[39], [40], lack of exploration accuracy and getting stuck in local optima [34], [39], [41], [42], [44], and low convergence rate [34], [35], [38]–[41], that need to be adequately addressed.

In this article, modified versions of WOA algorithm with/without fractional chaotic map, namely, the enhanced WOA (EWOA) and fractional chaotic EWOA (FC-EWOA), are proposed. In the proposed algorithms, to enhance the convergence of WOA, the population is efficiently divided into two equivalent subpopulations, and each agent updates its position in respect of the position of the best agent, so-called the leader, in its current subpopulation, the position of the other subpopulation's leader, and the position of the best neighboring agent. Due to the ergodic and non-repetition behaviours of chaotic maps, the combination of integer-order chaotic maps and meta-heuristic algorithms has proved to deliver significant improvements to the performance of algorithms [45], [46]. On the other hand, incorporation of fractional calculus with chaotic maps have enriched the dynamical behaviour of maps by demonstrating different distributions in comparison with integer-order counterparts [47]–[52]. According to the investigation results reported in the literature, the main superiorities of fractional-order chaotic maps compared with the integer-order chaotic maps can be summarized as (i) wider chaotic regions can be achieved due to the addition of fractional-order [50], (ii) more random chaotic sequences, more stability, and higher level of security are guaranteed [50], [51], and (iii) better ergodicity and distribution characteristic are illustrated [52]. In this context, researchers have deployed fractional chaotic maps to enhance the performance of optimization algorithms, such as fractional chaotic ensemble particle swarm optimizer [50] and fractional flower pollination algorithm [53]. Thus, in this study, incorporation of fractional-order variant of the chaos maps into the proposed EWOA is developed to boost its performance. Comparative investigations, along with different statistical analyzes are performed to testify the behaviour of the proposed algorithms through parameter identification of

isolated WDPS. According to the results achieved, the proposed strategies not only enhance the exploitation ability, but also expedite the convergence speed of the basic WOA.

This article is established into the following sections. The problem of WDPS identification is described in Section 2. The new enhanced fractional chaotic whale optimization algorithms are proposed in Section 3. Section 4 illustrates the comparative behaviour evaluation of the proposed algorithms through parameter identification of WDPS. Section 5 provides conclusions.

II. WDPS MODEL

A standalone hybrid WDPS is considered, consisting of static VAR compensator (SVC) which provides the required reactive power, isolated load, synchronous generator (SG), and induction generator (IG) driven by diesel engine and wind turbine (WT), respectively. As Fig. 1 depicts, the SG connected to the diesel generator (DG) form the diesel generator set, where it acts as a local grid for the wind system, which is formed by a connection of the IG and the WT.

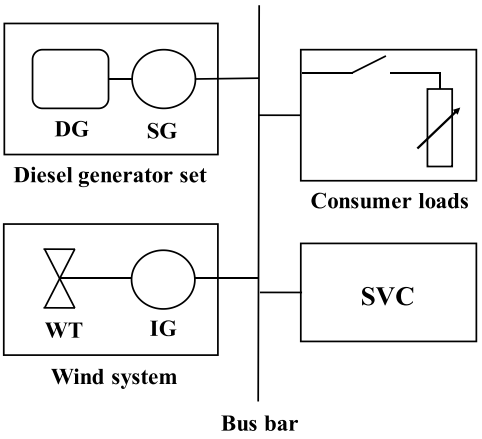

FIGURE 1. The block diagram of isolated WDPS.

The reactive-power balance of the system under steady-state condition can be expressed as follows [8], [54]:

$$Q_{\mathrm{SVC}} + Q_{\mathrm{SG}} = Q_{\mathrm{IG}} + Q_{\mathrm{L}} \tag{1}$$

where Q_{SG} and Q_{SVC} denote the reactive powers generated by DG and SVC, respectively; Q_{L} is the demanded reactive-power-load, and Q_{IG} is the required reactive power by the generator. It is assumed that the WDPS has a reactive power load change ΔQ_{L}. Thanks to the impact of the SVC and AVR controllers, due to the change in the system terminal voltage ΔV_t, the required reactive power will change, and also the reactive power generation system will increase as $\Delta Q_{\mathrm{SVC}} + \Delta Q_{\mathrm{SG}}$. Therefore, the net reactive power surplus in the system can be represented as [8]:

$$\Delta Q_{\mathrm{net}} = \Delta Q_{\mathrm{SVC}} + \Delta Q_{\mathrm{SG}} - \Delta Q_{\mathrm{IG}} - \Delta Q_{\mathrm{L}} \tag{2}$$

The reactive-power control transfer function diagram for the WDPS is depicted in Fig. 2. Accordingly, by assuming

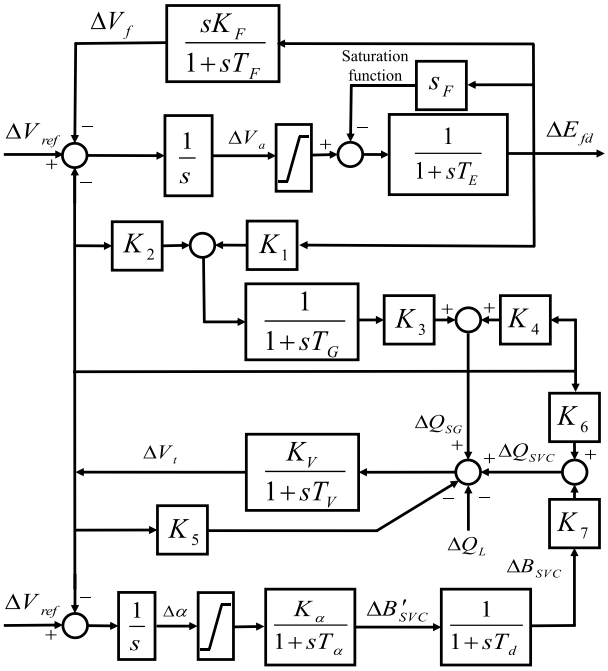

FIGURE 2. The reactive-power control transfer function diagram for the WDPS.

the existence of small perturbations, the complete linearized model of the system can be achieved as follows (see [55] for more details).

$$\frac{d\Delta E_{fd}}{dt} = -\frac{1}{T_E}\Delta E_{fd} + \frac{1}{T_E}\Delta V_a \tag{3-a}$$

$$\frac{d\Delta V_f}{dt} = \frac{K_F}{T_F T_E}\left[\Delta V_a - \Delta E_{fd}\right] - \frac{1}{T_F}\Delta V_f \tag{3-b}$$

$$\frac{d\Delta V_a}{dt} = \Delta V_{ref} - \left(\Delta V_f + \Delta V_t\right) \tag{3-c}$$

$$\frac{d\Delta E'_q}{dt} = \frac{K_1}{T_G}\Delta E_{fd} - \frac{1}{T_G}\Delta E'_q + \frac{K_2}{T_G}\Delta V_t \tag{3-d}$$

$$\frac{d\Delta B_{SVC}}{dt} = -\frac{1}{T_d}\Delta B_{SVC} + \frac{1}{T_d}\Delta B'_{SVC} \tag{3-e}$$

$$\frac{d\Delta B'_{SVC}}{dt} = -\frac{1}{T_\alpha}\Delta B'_{SVC} + \frac{K_\alpha}{T_\alpha}\Delta\alpha \tag{3-f}$$

$$\frac{d\Delta\alpha}{dt} = \left[\Delta V_{ref} - \Delta V_t\right] \tag{3-g}$$

$$\frac{d\Delta V_t}{dt} = \frac{K_3 K_V}{T_V}\Delta E'_q + \frac{K_7 K_V}{T_V}\Delta B_{SVC} + \frac{K_V K_4 + K_V K_6 - K_V K_5 - 1}{T_V}\Delta V_t - \frac{1}{T_V}\Delta Q_L \tag{3-h}$$

where ΔE_{fd} denotes the small changes in the SG exciter voltage, ΔV_a is the amplifier output voltage, T_E stands for the exciter time constant, ΔV_f is the feedback voltage, T_F and K_F denote the time constants and the stabilizer gain, respectively. ΔV_{ref} denotes the small changes in the reference voltage, T_G and $\Delta E'_q$ are the internal armature time constant and small changes in the voltage under transient condition, respectively, T_d represents the SVC average dead time of

zero crossing, and ΔB_{SVC} and $\Delta B'_{SVC}$ stand for the small deviations in the reactive susceptances of the SVC under steady-state and transient conditions, respectively. T_α is the thyristor firing delay time, $\Delta\alpha$ denotes the small thyristor firing angle changes, T_V and K_V show the terminal voltage time and gain constants, respectively, and K_α is the thyristor firing gain.

III. PROPOSED ENHANCED FRACTIONAL CHAOTIC WOA

A. THE BASIC WOA

The WOA is an interesting nature-inspired algorithm motivated by the hunting behavior of humpback whales [29]. This algorithm mimics the attacking mechanism of a swarm of whale individuals to solve optimization problems, where the position of each whale indicates the feasible solution. The WOA consists of three stages: (a) encircling the prey, (b) spiral bubble-net feeding maneuver, (c) search for the prey, where the first two phases represent the exploitation process, and the last phase represents the exploration. As the whales recognize the location of the prey, they dive deep and start creating bubble-nets in a spiral pattern around the prey and simultaneously swim-up to the surface. During the prey encircling phase, each whale encircles the target prey and maintains a candidate solution, and the best solution is determined. Correspondingly, other individuals update their positions with respect to the best search agent. This behavior at iteration t is represented as:

$$\vec{\Phi} = \left|\eta\vec{\Lambda}^*(t) - \vec{\Lambda}(t)\right| \tag{4}$$

$$\vec{\Lambda}(t+1) = \vec{\Lambda}^*(t) - \zeta\vec{\Phi} \tag{5}$$

where the symbol $|\cdot|$ denotes the absolute value, ζ and η represent the coefficient parameters, $\vec{\Lambda}$ and $\vec{\Lambda}^*$ denote the position vector of the current agent and the best solution acquired so far, respectively. The parameters η and ζ are also calculated as:

$$\zeta = \kappa\eta - \kappa \tag{6}$$

$$\eta = q\upsilon \tag{7}$$

where κ is the damping coefficient, which linearly decreases from 2 to 0 with respect to iteration number, q is a constant value, which is set to 2, and $\upsilon \in [0, 1]$ is a random value.

The bubble-net behavior consists of two strategies, namely, the shrinking encircling mechanism and the spiral position update. In the first approach, the coefficient parameter ζ varies in the range $[-\kappa, \kappa]$ and $\kappa \in [0, 2]$, thus, by setting random values for $\zeta \in [-1, 1]$ the new search agent can be located between its original position and the position of the current best agent. In the second approach, the agent's new position is updated regarding the position of the prey and the agent according to the following spiral equation:

$$\vec{\Lambda}(t+1) = \vec{\Phi}' e^{\delta\varepsilon}\cos(2\pi\varepsilon) + \vec{\Lambda}^*(t) \tag{8}$$

where the distance between the ith agent and the prey is computed by $\vec{\Phi}' = \left|\vec{\Lambda}^*(t) - \vec{\Lambda}(t)\right|$, the constant δ defines the shape of the logarithmic spiral, and $\varepsilon \in [-1, 1]$ is a random value. In order to simultaneously perform the shrinking circling together with the spiral-shape movement, a random probability coefficient is adopted that updates the position of agents during the optimization process by choosing between the following two mechanisms:

$$\vec{\Lambda}(t+1) = \begin{cases} \vec{\Lambda}^*(t) - \zeta\vec{\Phi} & if\ \psi < 0.5 \\ \vec{\Phi}' e^{\delta\varepsilon}\cos(2\pi\varepsilon) + \vec{\Lambda}^*(t) & if\ \psi \geq 0.5 \end{cases} \tag{9}$$

where $\psi \in [0, 1]$ is a random value.

In order to perform the exploration process, the search agents need to adequately far-off the best agent and try to search randomly through the search space. To this end, ζ is randomly chosen either greater than 1 or less than -1, and the agents update their positions regarding randomly chosen agents rather than the best agent so far. The mathematical behavior of the exploration process is expressed by:

$$\vec{\Phi} = \left|\eta\vec{\Lambda}_{rand}(t) - \vec{\Lambda}(t)\right| \tag{10}$$

$$\vec{\Lambda}(t+1) = \vec{\Lambda}_{rand}(t) - \zeta\vec{\Phi} \tag{11}$$

where $\vec{\Lambda}_{rand}$ refers to a randomly selected agent from the current population.

B. FRACTIONAL CHAOTIC MAPS

Chaos theory studies the behavior of iterated functions that return random values in each iteration. Chaotic functions are highly sensitive to initial conditions, such that any small difference in initial conditions yield to divergent in the generated sequence of values. The integration of chaotic functions into optimization algorithms have demonstrated promising improvements in the speed of convergence of the algorithms and the solutions diversity. Thus, they have been widely studied for global optimization and engineering problems [45], [46]. Different chaotic maps are introduced in the literature [56], due to their interesting characteristics such as a) the chaotic maps are generated by a deterministic dynamic rule, b) the time series is bounded between upper and lower limits, c) they act aperiodic, and d) the sequence is dependant to the initial condition.

Considering the above-mentioned characteristics, chaotic maps can effectively increase the exploration power of the stochastic search processes, which make them perfect replacements for the existing random generators. Thus, in this article, three fractional chaotic maps are embedded to adjust κ in the proposed EWOA algorithm, namely FC-EWOA. The fractional chaotic maps including the Fractional

Sine map [57], the Fractional Logistic map [57], and the Fractional Tent map [58], together with their relationships and distributions are listed in Table 1.

C. PROPOSED FC-EWOA

Although the WOA is an efficient optimization algorithm in dealing with global optimization and engineering problems [30]–[33], but yet, it has the main shortcoming that is premature convergence, which leads the algorithm to

TABLE 1. Fractional chaotic maps within the range (0, 1).

f	Map Name	Mathematical Representation	θ_0	Parameters
1	Fractional Logistic	$\theta_{t+1}=\theta_0+\frac{\sigma}{\Gamma(\varphi)}\sum_{j=1}^{t}\frac{\Gamma(t-j+\tau)}{\Gamma(t-j+1)}\theta_{j-1}\left(1-\theta_{j-1}\right)$	0.3	$\sigma=2.5$, $\tau=0.3$
2	Fractional Sine	$\theta_{t+1}=\theta_0+\frac{\sigma}{\Gamma(\tau)}\sum_{j=1}^{t}\frac{\Gamma(t-j+\tau)}{\Gamma(t-j+1)}\sin\left(\theta_{j-1}-1\right)$	0.3	$\sigma=3.8$, $\tau=0.8$
3	Fractional Tent	$\theta_{t+1}=\theta_0+\frac{1}{\Gamma(\tau)}\sum_{j=1}^{t}\frac{\Gamma(t-j+\tau)}{\Gamma(t-j+1)}\min\left((\sigma-1)\theta_{j-1},\sigma-(\sigma+1)\theta_{j-1}\right)$	0.3	$\sigma=1.9$, $\tau=0.6$

get trapped into local optima easily. Many studies have been addressed in the literature to overcome this deficiency [34]–[44]. In this article, enhanced whale optimization algorithms, namely EWOA and FC-EWOA, are proposed.

The EWOA consists of modifications to the position update procedure, which will be discussed, and the FC-EWOAs are modified versions of EWOA, which incorporate fractional chaotic maps into the search process of EWOA. Here, the proposed fractional chaotic EWOA algorithms are denoted by FC1-EWOA (with logistic map), FC2-EWOA (with sine map), and FC3-EWOA (with tent map). Through the exploitation process of WOA, each agent updates its position based on the position of the best agent, which reduces the diversity of the population, leading to a low convergence rate. The population is efficiently divided into two semi-independent subpopulations with the same number of agents, where the best agent in each subpopulation is determined. To address the convergence problem in WOA, the position of each agent is updated in terms of three factors, namely the best agent's position in its current subpopulation, the best agent's position in the other subpopulation, and the neighboring agent's position denoted by *nbest* that have better fitness than itself. This behavior can be expressed as follows:

$$\vec{\Phi}=\left|\eta_3\vec{\Lambda}_{nbest}(t)-\vec{\Lambda}(t)\right| + \left|\eta_2\vec{\Lambda}_2^*(t)-\vec{\Lambda}(t)\right|+\left|\eta_1\vec{\Lambda}_1^*(t)-\vec{\Lambda}(t)\right| \quad (12)$$

where $\vec{\Lambda}_1^*$ and $\vec{\Lambda}_2^*$ represent the position of the best agents in the current and the other subpopulation, respectively. $\vec{\Lambda}_{nbest}$ denotes the position of the neighboring agent with better fitness, and $\eta_i = q_i\upsilon$ are the coefficient parameters, where $\{q_1, q_2, q_3\} = \{2, 1, 0.5\}$. Therefore, we have:

$$\vec{\Lambda}(t+1)=\frac{1}{N}\sum_{i=1}^{N}\left(\vec{\Lambda}_i^*(t)-\zeta_i\vec{\Phi}\right),\quad N=2 \quad (13)$$

where the coefficient parameterζ_i is computed as:

$$\zeta_i=\kappa\eta_i-\kappa,\quad i=1,2 \quad (14)$$

Remark 1: The convergence speed of the algorithm through the exploitation process depends on the parameters q_1, q_2 and q_3. Higher values of q_1 result in faster movement of the agents towards $\vec{\Lambda}_1^*$ and less exploitation accuracy. On the other hand, although lower values of q_1 leads to better exploitation accuracy, the convergence rate would be reduced. Higher values of q_2 attracts the agents to move towards the other subpopulation ($\vec{\Lambda}_2^*$ specifically), while the current subpopulation has not been well-exploited. Therefore, lower values of q_2 decreases the impact of $\vec{\Lambda}_2^*$ on the agents' position update procedure, which reduces the diversity of the solutions. Similar to q_2, lower values of q_3 decreases the diversity of the solutions due to the lower impact of $\vec{\Lambda}_{nbest}$ on the agents' update procedure. Alternatively, higher values of q_3 increase the diversity, but the agents get misled, which reduces the convergence rate and the accuracy of the algorithm.

As it is apparent, the basic WOA and the proposed EWOA consist of several arbitrary selected variables that notably affect the algorithm performance. The most key variable is the linearly decreasing damping coefficient $\kappa \in [0, 2]$, which is a crucial factor in the convergence rate of FC-EWOA. Thus, here, this variable is chaotically tuned. In this regard, κ is chaotically varied between 0 and 2, instead of being linearly decreased with respect to the iteration number as follows:

$$(Q-\kappa)_f=\left(\kappa_l-\frac{t}{T}(\kappa_h-\kappa_l)\right)+NC_f \quad (15)$$

where $(Q-\kappa)_f$ represents the chaos damping coefficient that follows the distribution of the FC-maps stated in Table 1 with index $f \in \{1, 2, 3\}$, denoting the fractional chaotic maps, T and t are the number of the total and the current iterations, respectively. On the other hand, κ_h and κ_l are the upper and the lower values of κ, and NC_f is defined as:

$$NC_f=\frac{\left(F-Ch_f-\min\left(F-Ch_f\right)\right)(\vartheta-\rho)}{\max\left(F-Ch_f\right)-\min\left(F-Ch_f\right)}+\rho \quad (16)$$

where $F - Ch_f$ is the considered fractional chaotic map, $\min(F - Ch_f)$ and $\max(F - Ch_f)$ represent the minimum and the maximum distribution range of the fractional chaotic maps, respectively, and $\rho = 0.6$ and $\vartheta = 0.9$ are the normalization interval ranges.

In FC-EWOA, the position of each agent through the bubble-net procedure is calculated as:

$$\vec{\Lambda}(t+1)=\left\|\vec{\Phi}_{tot}\right\|_2 e^{\delta\varepsilon}\cos(2\pi\varepsilon)+\vec{\Lambda}_i^*(t),\quad i=1,2 \quad (17)$$

where $\vec{\Phi}_{tot}=\left(\vec{\Phi}_1,\vec{\Phi}_2\right)$ and $\vec{\Phi}_i=\left|\vec{\Lambda}_i^*(t)-\vec{\Lambda}(t)\right|$.

Similar to the basic WOA, in order to calculate the new position of the agents, the random probability coefficient $\psi \in [0, 1]$ is chosen between the shrinking circling and the spiral-shape movement.

As the exploitation process completes, the two subpopulations are merged into one population, and the best agent is evaluated. Consequently, the position of every agent can be updated in terms of the whole population, which leads to more random movements through the exploration process. The mathematical behavior of the exploration process is as stated in (10) and (11), with the chaos damping coefficient given in (15) instead of $\kappa \in [0, 2]$. In summary, the pseudo-code for the proposed FC-EWOA can be presented in Algorithm 1. Moreover, the flowchart of the FC-EWOA is depicted in Fig. 3.

IV. SIMULATION RESULTS AND DISCUSSIONS

In this section, comparative performance evaluations of the new algorithms are conducted through mathematical benchmark functions and parameter identification of isolated WDPS. In this regard, the comparisons are carried out with eight well-established meta-heuristic algorithms, including the GSA [58], the firefly algorithm (FA) [59], the grey wolf optimizer (GWO) [60], the bacterial foraging optimization (BFO) [61], the bat algorithm (BA) [62], the flower pollination algorithm (FPA) [63], the dragonfly algorithm (DA) [64], and the basic WOA [29]. The parameters settings of the optimization algorithms under comparison are tabulated in Table 2. For each algorithm, 100 independent runs are performed with a population size of 50. In the performance evaluation section, the dimension of all test problems is set to $D = 50$. Besides, the maximum number of function evaluations (NFEs) of $10,000 \times D$ and 20,000 are set as the stopping criteria for benchmark functions optimization and parameter identification evaluations, respectively.

TABLE 2. Parameter settings for the algorithms.

Algorithm	Parameters
GSA [58]	$a = 20, limit = 2, p = 5$
FA [59]	$\gamma = 0.9, \beta_0 = 1.8, \alpha = 0.25, \omega = 0.95$
GWO [60]	$c_{1,2} = [2.5 \sim 0.5], w = [0.9 \sim 0.4], N_n = 20$
BFO [61]	$N_{re} = 5, N_{ed} = 2, N_c = 10, \alpha = 0.2, P_{ed} = 0.25$
BA [62]	$\{\alpha, \gamma\} \in [0.9 - 0.975], \varepsilon \in [-1, 1], f \in [0, 2]$
FPA [63]	$p = 0.8, \gamma = 0.01, \lambda = 1.5$
DA [64]	$\omega \in [0.9 \sim 0.2], c = 0.1, a = 0.1, s = 0.1, e = 1, f = 1$
WOA [29]	$\delta = 10, \kappa \in [0, 2], \varepsilon \in [-1, 1]$
EWOA	$\delta = 10, \varepsilon \in [-1, 1], \kappa \in [0, 2]$
FC1-EWOA	$\delta = 10, \varepsilon \in [-1, 1], \kappa =$ Fractional Logistic map
FC2-EWOA	$\delta = 10, \varepsilon \in [-1, 1], \kappa =$ Fractional Sine map
FC3-EWOA	$\delta = 10, \varepsilon \in [-1, 1], \kappa =$ Fractional Tent map

A. PERFORMANCE EVALUATION

To testify the performance of the proposed algorithms, 8 problems adopted from the CEC2017 benchmark test suite are used as objective functions. The test problems are considered with various difficulty levels and categorized as unimodal functions, simple multimodal functions, hybrid functions, and composition functions with the search range of $[-100, 100]$, as illustrated in Table 3. The experimental results obtained by the algorithms are shown in Table 4, where standard deviation (S.D) represents the standard deviation, and the best minimum mean value achieved for each function is highlighted in bold.

The test results in Table 4 show that the proposed algorithms exhibit the best performance on all functions. FC1-EWOA performs significantly better than all other algorithms with 6 best results on $(f_2, f_3, f_4, f_6, f_7, f_8)$, followed by

Algorithm 1 Pseudo-Code for the Proposed FC-EWOA

```
Objective function f(x), x_i = (x_1, x_2, ..., x_d)
Set the position of whale individuals randomly;
Assess the fitness values for each individual;
NFE=NFE+1;
Divide the population into two subpopulations, and
 assign the leaders and members;
Λ* = the best search agent in each subpopulation;
while (stopping criterion)
   for every search agent
   Update the chaos damping coefficient using (15);
  Update ζ, η, ε, and ψ;
  Evaluate Φ using (12);
  if-1 ψ < 0.5
     if-2 |ζ| < 1
          Update the current search agent's position
          using (13);
          NFE=NFE+1;
     elseif-2 |ζ| ≥ 1
          Merge the subpopulations into one
          population;
          Update the current search agent's position
           using (10) and (11) with chaos damping
          coefficient (15);
          NFE=NFE+1;
          Rank the whale agents and determine the
           current best agent (Λ*);
          Define the subpopulations and assign the
           leaders and members;
     end if-2
  elseif-1 ψ ≥ 0.5
       Update the position of the current search agent
        using (17);
       NFE=NFE+1;
       end if-1
    end for
    Rank the whale agents;
    Determine the current best agent (Λ*) in each
     subpopulation;
end while
```

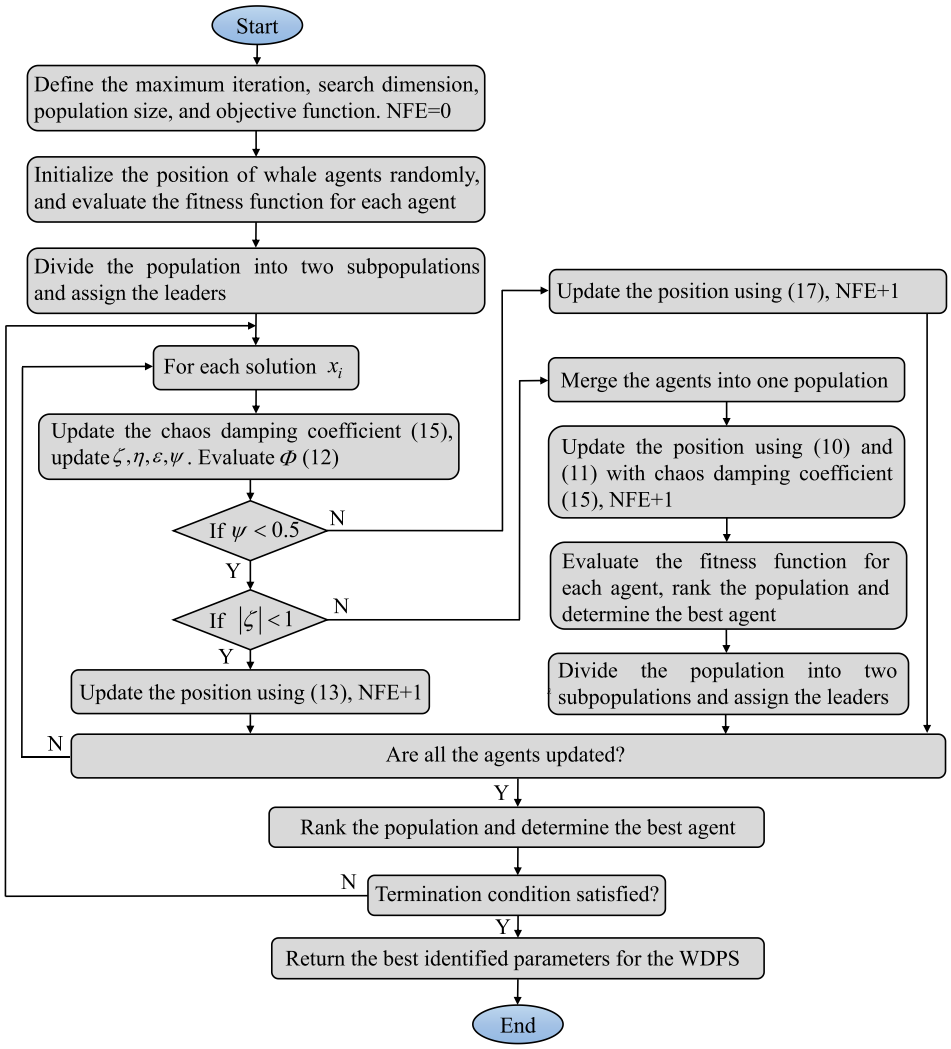

FIGURE 3. The proposed FC-EWOA flowchart.

TABLE 3. The definition of considered CEC2017 benchmark problems.

Type	f	Functions
Unimodal Function	1	Shifted and Rotated Bent Cigar Function
	2	Shifted and Rotated Sum of Different Power Function
Simple Multimodal Function	3	Shifted and Rotated Rosenbrock's Function
	4	Shifted and Rotated Levy Function
Hybrid Function	5	Hybrid Function 1 (N=3)
	6	Hybrid Function 7 (N=5)
Composition Function	7	Composition Function 4 (N=4)
	8	Composition Function 8 (N=6)

FC2-EWOA with 2 best results on (f_1, f_5). From Table 4 and based on the overall performance ranking of all algorithms, FC1-EWOA is the best algorithm, followed successively by FC2-EWOA, FC3-EWOA, EWOA, GWO, WOA, GSA, FA, BFO, BA, FPA, and DA.

For better demonstration of performance comparisons, the convergence curves of average best solutions of the proposed algorithms and other algorithms on the 8 selected benchmark problems are depicted in Fig. 4. According to Fig. 4, the proposed EWOA and its fractional versions demonstrate the fastest rates of convergence throughout the early stages in comparison to other methods, which illustrates one of the superiorities of the proposed algorithms. Another superiority is their capability to deal with multimodal, hybrid, and composition functions. As is clearly shown in Fig. 4, the proposed algorithms maintain excellent search abilities both globally and locally, while other algorithms are mostly gotten trapped into local optimum prematurely. Besides, although in the first stages, the convergence of FC1-EWOA is relatively slower than the other three proposed algorithms, in 6 problems it surpasses them in the middle stages.

To sum up, as stated in Table 4 and can be seen in Fig. 4, the proposed algorithms demonstrate the best performance in terms of convergence rate and optimization, followed by

TABLE 4. Experimental results of considered CEC2017 benchmark functions with D=50.

Algorithm		f_1	f_2	f_3	f_4	f_5	f_6	f_7	f_8
GSA	Mean	1.67E+02	1.38E+05	2.38E+02	2.66E+01	3.87E+01	2.28E+03	2.57E+03	2.97E+02
	S.D.	3.15E+03	2.23E+05	1.36E+02	1.75E+01	2.38E+01	1.50E+02	1.61E+02	2.38E+01
FA	Mean	1.88E+02	2.93E+06	4.63E+02	2.54E+01	4.10E+01	2.30E+03	1.03E+03	2.67E+02
	S.D	2.46E+02	2.42E+05	2.37E+01	1.39E+00	1.08E+01	1.78E+02	3.51E+02	8.49E+01
GWO	Mean	2.95E+03	1.31E+05	2.41E+02	2.12E+01	2.75E+01	1.43E+03	3.23E+02	1.78E+02
	S.D	1.58E+03	3.41E+06	1.38E+02	1.32E+02	8.36E+00	8.11E+02	4.36E+01	2.03E+01
BFO	Mean	3.94E+02	4.90E+05	2.67E+02	3.80E+02	5.19E+02	2.86E+03	1.47E+03	2.85E+02
	S.D	1.39E+02	2.17E+05	2.11E+01	8.98E+01	1.43E+02	6.83E+01	8.74E+02	2.75E+01
BA	Mean	3.75E+03	3.17E+06	1.74E+03	2.46E+02	4.87E+01	4.38E+03	5.39E+03	3.16E+03
	S.D	5.14E+02	4.65E+05	2.16E+02	3.61E+02	2.09E+01	2.74E+02	2.07E+02	2.48E+02
FPA	Mean	3.46E+03	1.68E+07	2.41E+03	2.57E+02	4.66E+02	4.94E+03	4.68E+03	3.28E+03
	S.D	2.14E+03	1.13E+06	2.24E+02	1.39E+03	1.41E+01	1.38E+03	2.84E+02	1.17E+02
DA	Mean	5.16E+03	2.49E+07	3.39E+03	5.48E+02	5.74E+02	5.13E+03	6.94E+03	6.61E+03
	S.D	2.20E+03	2.74E+06	2.07E+02	2.46E+02	1.04E+02	2.38E+03	2.36E+02	3.29E+02
WOA	Mean	2.13E+02	2.18E+05	1.68E+02	2.18E+01	3.38E+01	2.12E+03	2.37E+02	2.05E+02
	S.D	4.06E+01	1.48E+05	2.23E+01	2.74E+00	2.38E+00	1.18E+02	1.16E+01	6.14E+01
EWOA	Mean	1.51E+01	3.16E+04	1.81E+01	1.62E-01	1.34E+01	3.15E+02	2.48E+01	1.37E+01
	S.D	3.27E+01	2.48E+04	1.79E+00	2.03E-02	2.68E+00	2.84E+01	3.16E+01	4.58E+01
FC1-EWOA	Mean	1.15E+01	**1.27E+04**	**1.32E+01**	**1.25E-02**	1.15E+01	**2.22E+01**	**1.05E+01**	**1.00E+01**
	S.D	1.03E+00	2.44E+02	1.14E+00	2.60E-04	1.74E+00	2.26E-01	2.55E+00	2.15E+00
FC2-EWOA	Mean	**1.11E+01**	1.37E+04	1.45E+01	1.34E-02	**1.12E+01**	2.33E+01	1.16E+01	1.21E+01
	S.D	2.18E+00	2.41E+02	1.41E+00	2.31E-04	1.75E+00	2.78E+00	2.29E+00	1.29E+01
FC3-EWOA	Mean	1.37E+01	1.34E+04	1.36E+01	1.49E-02	1.24E+01	2.36E+01	1.24E+01	1.34E+01
	S.D	2.30E+00	2.37E+02	1.26E+00	2.40E-04	2.04E+00	3.28E-01	2.61E+00	2.31E+00

GWO, WOA, GSA, and FA, which deliver better results in comparison with other methods under study.

B. PARAMETER IDENTIFICATION OF WDPS

The parameter identification of isolated WDPS is conducted in this sub-section. This problem is transformed as an optimization problem, where the goal is to identify the parameters such that the difference between the actual and current data is minimized. Therefore, we consider the following objective functions, which are the mean square error (MSE), the mean absolute error (MAE), the root mean square error (RMSE), respectively.

$$MSE = \frac{1}{N}\sum_{i=1}^{N} E_i\left(\Delta Q_{SG}, \Delta Q_{SVC}, \Delta Q_{IG}, x\right)^2 \tag{18}$$

$$MAE = \frac{1}{N}\sum_{i=1}^{N} E_i\left|\Delta Q_{SG}, \Delta Q_{SVC}, \Delta Q_{IG}, x\right| \tag{19}$$

$$MSE = \left[\frac{1}{N}\sum_{i=1}^{N} E_i\left(\Delta Q_{SG}, \Delta Q_{SVC}, \Delta Q_{IG}, x\right)^2\right]^{1/2} \tag{20}$$

where x is the solution vector consisting of sixteen identified parameters, $E(\Delta Q_{SG}) = (\Delta Q_{SG,\text{actual}} - \Delta Q_{SG,\text{identified}})$, $E(\Delta Q_{SVC}) = (\Delta Q_{SVC,\text{actual}} - \Delta Q_{SVC,\text{identified}})$, and $E(\Delta Q_{IG}) = (\Delta Q_{IG,\text{actual}} - \Delta Q_{IG,\text{identified}})$.

In Table 5, we list the actual parameters values and the search ranges of unknown parameters for the WDPS. The comparative performance evaluation results of the proposed methods for the WDPS parameter identification problem with respect to other algorithms are presented in Tables 6 and 7. According to Table 6, the proposed EWOA and FC-EWOA algorithms can obtain more accurate parameters for the WDPS system.

TABLE 5. The parameters values and range (lower and upper boundaries).

Param.	LB	UB	Value	Param.	LB	UB	Value
K_1	0	5	0.1500	T_v	0	5	1.0600E-04
K_2	0	5	0.7932	K_v	0	5	1.0000
K_3	0	20	6.2214	T_G	0	5	0.7500
K_4	-20	20	-7.3589	T_E	0	5	0.5500
K_5	0	5	0.1260	T_F	0	5	0.7150
K_6	0	5	1.4780	K_F	0	5	0.5000
K_7	0	5	1.0000	T_α	0	5	0.0050
T_d	0	5	0.0017	K_α	0	5	0.4464

Table 7 shows the applied error metrics together with their corresponding standard deviation, such that the best results indicating the minimum error is emphasized in bold. From Table 7, we observe that the error values obtained by the proposed EWOA algorithms are remarkably less than other methods.

Besides, the FC1-EWOA demonstrates the best performance among all algorithms by achieving the least possible identification error value in terms of MAE, RMSE, and MSE. Results manifest the superiority of the proposed EWOA and FC-EWOA algorithms, yielding outstanding parameter identification performance with 16 accurate identified parameters achieved out of 16 parameters, followed by GWO and WOA with 3 and 2 accurate parameters, respectively.

It is worth pointing out that the results accuracy is computed and presented to eight and four decimal places, respectively. To intuitively compare and analyze the quality of the

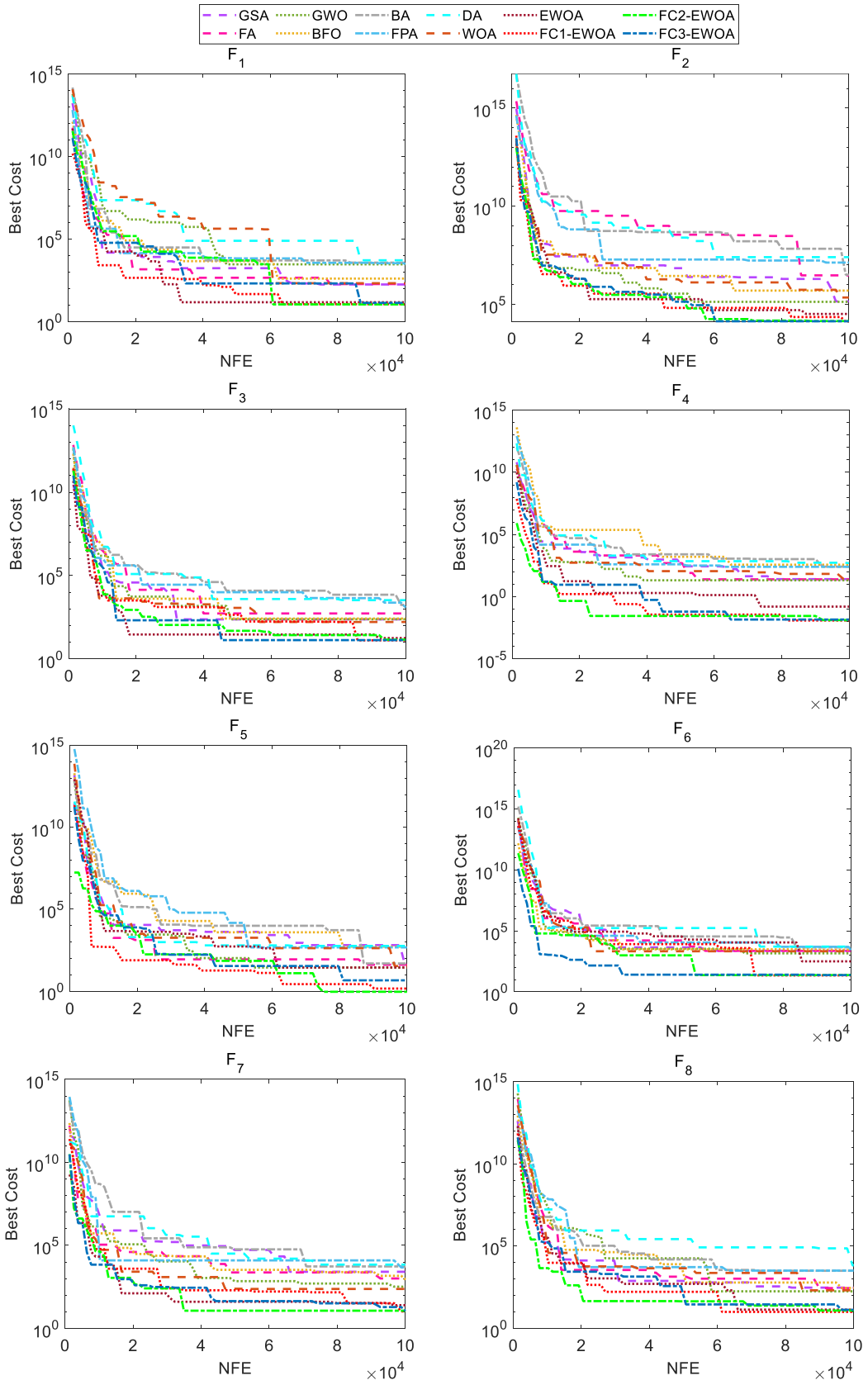

FIGURE 4. The convergence curves of the average best solutions obtained by algorithms.

TABLE 6. Parameters identification comparison.

Parameter	K_1	K_2	K_3	K_4	K_5	K_6	K_7	T_d
GSA	0.1418	0.7670	6.1218	-7.3330	0.1168	1.4575	0.9534	0.0022
FA	0.1395	0.7679	6.1256	-7.3317	0.1151	1.4561	1.0310	0.0025
GWO	0.1438	0.7851	6.1684	-7.3416	0.1260	1.4638	1.0284	0.0017
BFO	0.1389	0.7653	6.0816	-7.3308	0.1130	1.4511	0.9516	0.0008
BA	0.1365	0.7558	6.0153	-7.3107	0.1109	1.4326	0.9358	0.0004
FPA	0.1378	0.7634	6.0210	-7.3260	0.1118	1.4440	1.0413	0.0031
DA	0.1340	0.7510	6.0137	-7.2841	0.1109	1.4206	0.9379	0.0031
WOA	0.1421	0.7720	6.1420	-7.3350	0.1208	1.4610	0.9681	0.0017
EWOA	0.1500	0.7932	6.2214	-7.3589	0.1260	1.4780	1.0000	0.0017
FC1-EWOA	0.1500	0.7932	6.2214	-7.3589	0.1260	1.4780	1.0000	0.0017
FC2-EWOA	0.1500	0.7932	6.2214	-7.3589	0.1260	1.4780	1.0000	0.0017
FC3-EWOA	0.1500	0.7932	6.2214	-7.3589	0.1260	1.4780	1.0000	0.0017

Parameter	T_v	K_v	T_G	T_E	T_F	K_F	T_α	K_α
GSA	1.4114E-04	0.9017	0.7356	0.5062	0.7026	0.4741	0.0061	0.4320
FA	8.1670E-05	0.9146	0.7316	0.4938	0.7019	0.4723	0.0036	0.4301
GWO	1.2912E-04	1.0761	0.7500	0.5211	0.7087	0.4816	0.0042	0.4412
BFO	7.9804E-05	1.1025	0.7318	0.4951	0.7005	0.4716	0.0067	0.4316
BA	6.5841E-05	1.1158	0.7206	0.4738	0.6946	0.4670	0.0074	0.4234
FPA	7.6701E-05	1.1123	0.7284	0.4860	0.7000	0.4703	0.0031	0.4250
DA	6.1059E-05	0.8876	0.7238	0.4703	0.6910	0.4666	0.0028	0.4228
WOA	1.3660E-04	1.0884	0.7390	0.5107	0.7150	0.4820	0.0040	0.4384
EWOA	1.0600E-04	1.0000	0.7500	0.5500	0.7150	0.5000	0.0050	0.4464
FC1-EWOA	1.0600E-04	1.0000	0.7500	0.5500	0.7150	0.5000	0.0050	0.4464
FC2-EWOA	1.0600E-04	1.0000	0.7500	0.5500	0.7150	0.5000	0.0050	0.4464
FC3-EWOA	1.0600E-04	1.0000	0.7500	0.5500	0.7150	0.5000	0.0050	0.4464

TABLE 7. Parameters identification comparison.

Error Value	MAE	S.D	RMSE	S.D	MSE	S.D
GSA	1.5940E-02	3.0354E-04	2.0067E-01	4.6684E-03	6.1678E-04	1.5115E-06
FA	1.3863E-02	4.3005E-04	2.0265E-01	6.4871E-04	2.2354E-04	2.1625E-07
GWO	3.5716E-03	2.2160E-05	6.1628E-02	2.2168E-04	3.1396E-05	5.1356E-08
BFO	2.8400E-02	1.3459E-03	5.8150E-01	5.4820E-03	2.0014E-03	2.2135E-05
BA	1.0845E-01	2.2684E-03	3.0625E-01	2.7921E-03	3.3610E-03	1.3418E-05
FPA	5.6904E-02	4.1035E-04	1.6700E-01	4.8152E-04	5.1654E-04	2.2165E-07
DA	2.5684E-01	2.2227E-02	6.3851E-01	1.6840E-03	7.8208E-05	2.1147E-07
WOA	1.2655E-03	2.2135E-05	1.7000E-02	4.2965E-04	4.0842E-05	1.8859E-09
EWOA	1.6284E-21	1.8537E-25	6.4733E-20	2.3685E-22	2.8810E-26	3.1680E-30
FC1-EWOA	**0.0000E+00**	0.0000E+00	**0.0000E+00**	0.0000E+00	**0.0000E+00**	0.0000E+00
FC2-EWOA	1.2326E-32	0.0000E+00	2.3685E-30	0.0000E+00	**0.0000E+00**	0.0000E+00
FC3-EWOA	7.8886E-31	0.0000E+00	6.4165E-30	0.0000E+00	**0.0000E+00**	0.0000E+00

solutions from a statistical point of view, Table 8 provides the comparative Friedman test [65] results, where the column "Rank" denotes the performance order of the algorithms. The results regarding the Friedman test show the superiority of the proposed algorithms in comparison with others, which verifies the above conclusion again. In order to test the conformity between the real and the estimated WDPS parameters, the transient responses of Q_{SG}, Q_{SVC}, and Q_{IG} for a 5% step increment in the reactive power load are illustrated in Figs. 5-7. The results reveal the accuracy and quality of the estimated parameters and simultaneously validate the feasibility of the proposed algorithms. According to the results, the largest deviations between the transient responses with the actual and the estimated parameters are demonstrated by BA.

In addition, although the GWO and WOA algorithms demonstrate better fitting results compared with BA, yet, the accuracy of their results is markedly less than the proposed EWOA and FC-EWOA, which again, indicates

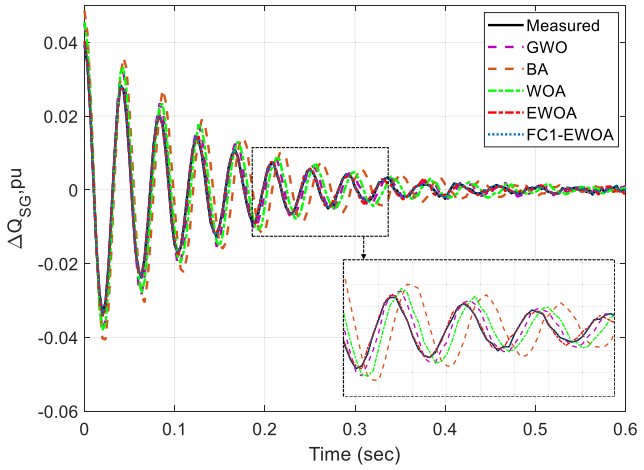

FIGURE 5. The DG-generated reactive power with a 5% step increment in the load reactive-power (transient response).

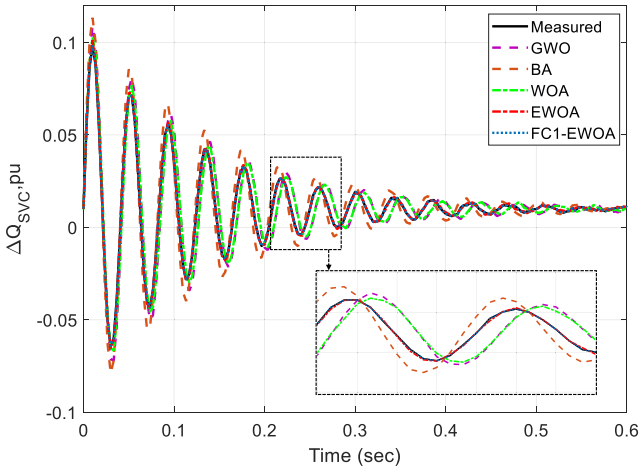

FIGURE 6. The SVC-generated reactive power with a 5% step increment in the load reactive-power (transient response).

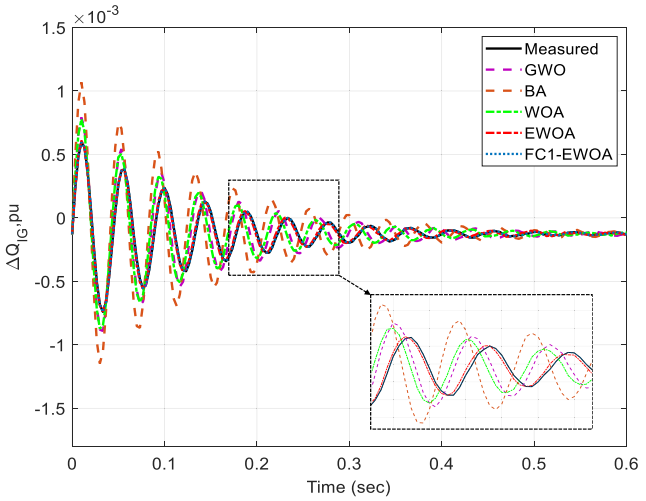

FIGURE 7. The generator-required reactive power with a 5% step increment in the load reactive-power (transient response).

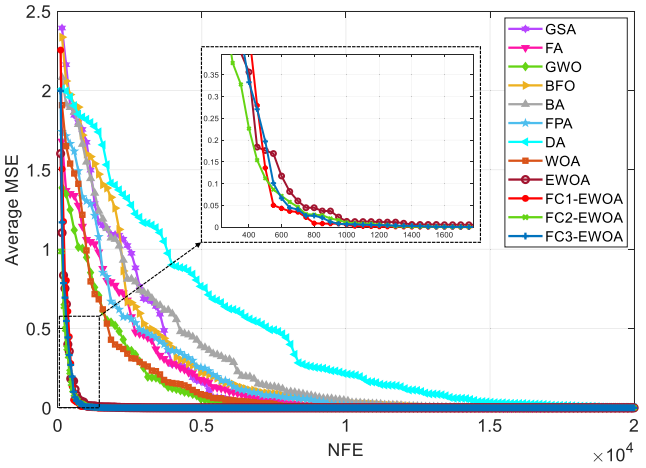

FIGURE 8. Average convergence curve of the objective function.

the remarkable performance of the proposed algorithms. Fig. 8 depicts the average convergence profile of the objective function for the proposed algorithms in comparison with other methods. From Fig. 8, it can be observed that the proposed EWOA and FC-EWOA algorithms demonstrate significantly higher convergence speed than others.

Accordingly, the proposed FC-EWA algorithms converge to the minimum value of MSE within 2000 function evaluations, followed by the proposed EWOA with 3600 function evaluations, indicating the exceptional performance of the proposed algorithms. On the other hand, although other methods could not achieve the minimum MSE value, still GWO, WOA, GSA, and FA demonstrated more desirable performance compared to BFO, FPA, BA, and DA.

The convergence rates of the WDPS parameters are depicted in Fig. 9, yielding more searching accuracy and faster convergence speed of the proposed algorithms in contrast with other algorithms. The aforementioned comparisons demonstrate that utilizing the proposed strategy presented in subsection 3.3 and embedding the FC-maps with the proposed algorithm affects the accuracy and enhances the performance of the basic WOA.

TABLE 8. Friedman statistical test results.

Algorithm	Score	Rank
GSA	5.1664	8
FA	5.0168	7
GWO	4.4850	5
BFO	5.4990	9
BA	6.5758	11
FPA	6.1699	10
DA	7.1200	12
WOA	4.9782	6
EWOA	1.1480	4
FC1-EWOA	1.0000	1
FC2-EWOA	1.0125	2
FC3-EWOA	1.0178	3

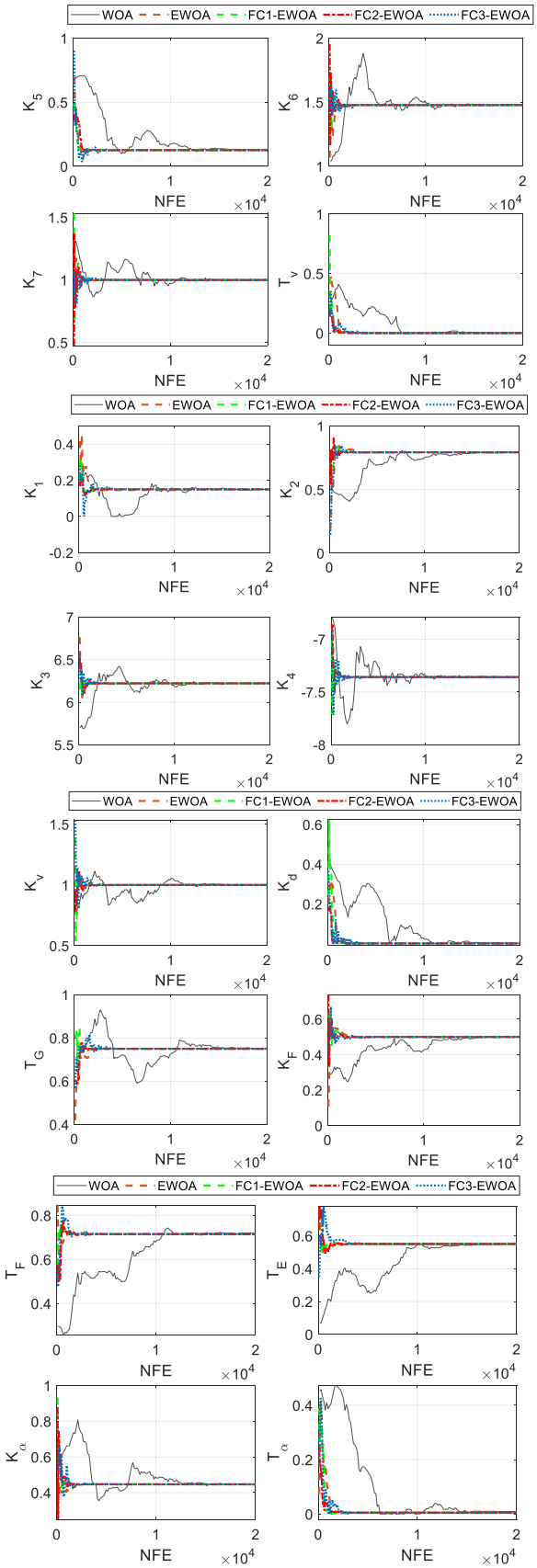

FIGURE 9. Convergence rate of the WDPS parameters.

V. CONCLUSION

Accurate modelling and appropriate controller design for the isolated WDPS require accurate identification of the model parameters. For this purpose and aiming at the main disadvantage of the whale optimization algorithm, which is premature convergence, four novel enhanced WOA algorithms are introduced. The proposed EWOA develops the position update procedure of WOA such that more accurate exploitation behavior is achieved. Besides, to enhance the performance of EWOA in terms of accuracy, three different fractional chaotic maps are taken into account in the search process of WOA. Efficiency and superiority of the proposed algorithms are validated via parameter identification of WDPS in comparison with other algorithms. Results confirm the remarkable performance of the proposed algorithms with respect to solution precision and speed of convergence.

REFERENCES

[1] A. Qazi, F. Hussain, N. A. Rahim, G. Hardaker, D. Alghazzawi, K. Shaban, and K. Haruna, "Towards sustainable energy: A systematic review of renewable energy sources, technologies, and public opinions," *IEEE Access*, vol. 7, pp. 63837–63851, 2019.

[2] B. Li, X. Mo, and B. Chen, "Direct control strategy of real-time tracking power generation plan for wind power and battery energy storage combined system," *IEEE Access*, vol. 7, pp. 147169–147178, 2019.

[3] Y. Gu, Y. Huang, Q. Wu, C. Li, H. Zhao, and Y. Zhan, "Isolation and protection of the motor-generator pair system for fault ride-through of renewable energy generation systems," *IEEE Access*, vol. 8, pp. 13251–13258, 2020.

[4] J. Aghaei, M. Barani, M. Shafie-khah, A. A. S. de la Nieta, and J. P. S. Catalao, "Risk-constrained offering strategy for aggregated hybrid power plant including wind power producer and demand response provider," *IEEE Trans. Sustain. Energy*, vol. 7, no. 2, pp. 513–525, Apr. 2016.

[5] S. Tao, L. Zhao, K. Liao, and Y. Liu, "Probability assessment of characteristics of sub-synchronous oscillation in D-PMSG-based wind power generation system," *IEEE Access*, vol. 7, pp. 133159–133169, 2019.

[6] Y. Mi, C. Ma, Y. Fu, C. Wang, P. Wang, and P. C. Loh, "The SVC additional adaptive voltage controller of isolated wind-diesel power system based on double sliding-mode optimal strategy," *IEEE Trans. Sustain. Energy*, vol. 9, no. 1, pp. 24–34, Jan. 2018.

[7] Y. Song, L. Liang, and M. Tan, "Neuroadaptive power tracking control of wind farms under uncertain power demands," *IEEE Trans. Ind. Electron.*, vol. 64, no. 9, pp. 7071–7078, Sep. 2017.

[8] R. C. Bansal, "Automatic reactive-power control of isolated wind–diesel hybrid power systems," *IEEE Trans. Ind. Electron.*, vol. 53, no. 4, pp. 1116–1126, Jun. 2006.

[9] H. Modares, A. Alfi, and M.-M. Fateh, "Parameter identification of chaotic dynamic systems through an improved particle swarm optimization," *Expert Syst. Appl.*, vol. 37, no. 5, pp. 3714–3720, May 2010.

[10] S. Ruder, "An overview of gradient descent optimization algorithms," 2016, *arXiv:1609.04747*. [Online]. Available: http://arxiv.org/abs/1609.04747

[11] B. Sereeter, C. Vuik, and C. Witteveen, "On a comparison of Newton–Raphson solvers for power flow problems," *J. Comput. Appl. Math.*, vol. 360, pp. 157–169, Nov. 2019.

[12] A. A. El-Fergany, H. M. Hasanien, and A. M. Agwa, "Semi-empirical PEM fuel cells model using whale optimization algorithm," *Energy Convers. Manage.*, vol. 201, Dec. 2019, Art. no. 112197.

[13] L. Liu, L. Shan, Y. Dai, C. Liu, and Z. Qi, "A modified quantum bacterial foraging algorithm for parameters identification of fractional-order system," *IEEE Access*, vol. 6, pp. 6610–6619, 2018.

[14] Z. Chen, X. Yuan, H. Tian, and B. Ji, "Improved gravitational search algorithm for parameter identification of water turbine regulation system," *Energy Convers. Manage.*, vol. 78, pp. 306–315, Feb. 2014.

[15] C. Li and J. Zhou, "Parameters identification of hydraulic turbine governing system using improved gravitational search algorithm," *Energy Convers. Manage.*, vol. 52, no. 1, pp. 374–381, Jan. 2011.

[16] H. Modares, A. Alfi, and M.-B. N. Sistani, "Parameter estimation of bilinear systems based on an adaptive particle swarm optimization," *Eng. Appl. Artif. Intell.*, vol. 23, no. 7, pp. 1105–1111, Oct. 2010.
[17] T. Tian, C. Liu, Q. Guo, Y. Yuan, W. Li, and Q. Yan, "An improved ant lion optimization algorithm and its application in hydraulic turbine governing system parameter identification," *Energies*, vol. 11, no. 1, p. 95, Jan. 2018.
[18] C. Li, L. Chang, Z. Huang, Y. Liu, and N. Zhang, "Parameter identification of a nonlinear model of hydraulic turbine governing system with an elastic water hammer based on a modified gravitational search algorithm," *Eng. Appl. Artif. Intell.*, vol. 50, pp. 177–191, Apr. 2016.
[19] B. Yang, J. Wang, X. Zhang, T. Yu, W. Yao, H. Shu, F. Zeng, and L. Sun, "Comprehensive overview of meta-heuristic algorithm applications on PV cell parameter identification," *Energy Convers. Manage.*, vol. 208, Mar. 2020, Art. no. 112595.
[20] G. Xiong, J. Zhang, D. Shi, and Y. He, "Parameter extraction of solar photovoltaic models using an improved whale optimization algorithm," *Energy Convers. Manage.*, vol. 174, pp. 388–405, Oct. 2018.
[21] Q. Hao, Z. Zhou, Z. Wei, and G. Chen, "Parameters identification of photovoltaic models using a multi-strategy Success-History-Based adaptive differential evolution," *IEEE Access*, vol. 8, pp. 35979–35994, 2020.
[22] L. Guo, Z. Meng, Y. Sun, and L. Wang, "Parameter identification and sensitivity analysis of solar cell models with cat swarm optimization algorithm," *Energy Convers. Manage.*, vol. 108, pp. 520–528, Jan. 2016.
[23] K. Yu, J. J. Liang, B. Y. Qu, X. Chen, and H. Wang, "Parameters identification of photovoltaic models using an improved JAYA optimization algorithm," *Energy Convers. Manage.*, vol. 150, pp. 742–753, Oct. 2017.
[24] M. H. Qais, H. M. Hasanien, and S. Alghuwainem, "Identification of electrical parameters for three-diode photovoltaic model using analytical and sunflower optimization algorithm," *Appl. Energy*, vol. 250, pp. 109–117, Sep. 2019.
[25] Y. Mousavi and A. Alfi, "Fractional calculus-based firefly algorithm applied to parameter estimation of chaotic systems," *Chaos, Solitons Fractals*, vol. 114, pp. 202–215, Sep. 2018.
[26] F. Pazhoohesh, S. Hasanvand, and Y. Mousavi, "Optimal harmonic reduction approach for PWM AC–AC converter using nested memetic algorithm," *Soft Comput.*, vol. 21, no. 10, pp. 2761–2776, May 2017.
[27] A. Arab and Y. Mousavi, "Optimal control of wheeled mobile robots: From simulation to real world," in *Proc. Amer. Control Conf.*, Denver, CO, USA, Jul. 2020, pp. 583–589.
[28] Y. Mousavi and A. Alfi, "A memetic algorithm applied to trajectory control by tuning of fractional order proportional-integral-derivative controllers," *Appl. Soft Comput.*, vol. 36, pp. 599–617, Nov. 2015.
[29] S. Mirjalili and A. Lewis, "The whale optimization algorithm," *Adv. Eng. Softw.*, vol. 95, pp. 51–67, May 2016.
[30] G. Hou, L. Gong, Z. Yang, and J. Zhang, "Multi-objective economic model predictive control for gas turbine system based on quantum simultaneous whale optimization algorithm," *Energy Convers. Manage.*, vol. 207, Mar. 2020, Art. no. 112498.
[31] M. A. E. Aziz, A. A. Ewees, and A. E. Hassanien, "Whale optimization algorithm and moth-flame optimization for multilevel thresholding image segmentation," *Expert Syst. Appl.*, vol. 83, pp. 242–256, Oct. 2017.
[32] F. S. Gharehchopogh and H. Gholizadeh, "A comprehensive survey: Whale optimization algorithm and its applications," *Swarm Evol. Comput.*, vol. 48 pp. 1–24, Aug. 2019.
[33] Q. Zhang and L. Liu, "Whale optimization algorithm based on lamarckian learning for global optimization problems," *IEEE Access*, vol. 7, pp. 36642–36666, 2019.
[34] A. Got, A. Moussaoui, and D. Zouache, "A guided population archive whale optimization algorithm for solving multiobjective optimization problems," *Expert Syst. Appl.*, vol. 141, Mar. 2020, Art. no. 112972.
[35] Y. Sun, X. Wang, Y. Chen, and Z. Liu, "A modified whale optimization algorithm for large-scale global optimization problems," *Expert Syst. Appl.*, vol. 114, pp. 563–577, Dec. 2018.
[36] W. Long, T. Wu, J. Jiao, M. Tang, and M. Xu, "Refraction-learning-based whale optimization algorithm for high-dimensional problems and parameter estimation of PV model," *Eng. Appl. Artif. Intell.*, vol. 89, Mar. 2020, Art. no. 103457.
[37] Y. Sun, T. Yang, and Z. Liu, "A whale optimization algorithm based on quadratic interpolation for high-dimensional global optimization problems," *Appl. Soft Comput.*, vol. 85, Dec. 2019, Art. no. 105744.
[38] W. Guo, T. Liu, F. Dai, and P. Xu, "An improved whale optimization algorithm for forecasting water resources demand," *Appl. Soft Comput.*, vol. 86, Jan. 2020, Art. no. 105925.
[39] M. H. Qais, H. M. Hasanien, and S. Alghuwainem, "Enhanced whale optimization algorithm for maximum power point tracking of variable-speed wind generators," *Appl. Soft Comput.*, vol. 86, Jan. 2020, Art. no. 105937.
[40] Y. Li, T. Han, H. Zhao, and H. Gao, "An adaptive whale optimization algorithm using Gaussian distribution strategies and its application in heterogeneous UCAVs task allocation," *IEEE Access*, vol. 7, pp. 110138–110158, 2019.
[41] M. Abd Elaziz and D. Oliva, "Parameter estimation of solar cells diode models by an improved opposition-based whale optimization algorithm," *Energy Convers. Manage.*, vol. 171, pp. 1843–1859, Sep. 2018.
[42] M. Abdel-Basset, G. Manogaran, D. El-Shahat, and S. Mirjalili, "Integrating the whale algorithm with tabu search for quadratic assignment problem: A new approach for locating hospital departments," *Appl. Soft Comput.*, vol. 73, pp. 530–546, Dec. 2018.
[43] Y. Cao, Y. Li, G. Zhang, K. Jermsittiparsert, and M. Nasseri, "An efficient terminal voltage control for PEMFC based on an improved version of whale optimization algorithm," *Energy Rep.*, vol. 6, pp. 530–542, Nov. 2020.
[44] W. Qiao, Z. Yang, Z. Kang, and Z. Pan, "Short-term natural gas consumption prediction based on volterra adaptive filter and improved whale optimization algorithm," *Eng. Appl. Artif. Intell.*, vol. 87, Jan. 2020, Art. no. 103323.
[45] K. Chen, F. Zhou, and A. Liu, "Chaotic dynamic weight particle swarm optimization for numerical function optimization," *Knowl.-Based Syst.*, vol. 139, pp. 23–40, Jan. 2018.
[46] X. Yuan, P. Wang, Y. Yuan, Y. Huang, and X. Zhang, "A new quantum inspired chaotic artificial bee colony algorithm for optimal power flow problem," *Energy Convers. Manage.*, vol. 100, pp. 1–9, Aug. 2015.
[47] A. Deshpande and V. DAFTARDAR-GEJJI, "Chaos in discrete fractional difference equations," *Pramana*, vol. 87, no. 4, p. 49, Oct. 2016.
[48] G.-C. Wu and D. Baleanu, "Discrete fractional logistic map and its chaos," *Nonlinear Dyn.*, vol. 75, nos. 1–2, pp. 283–287, Jan. 2014.
[49] Y. Peng, K. Sun, S. He, and L. Wang, "Comments on 'discrete fractional logistic map and its chaos' [nonlinear Dyn. 75, 283–287 (2014)]," *Nonlinear Dyn.*, vol. 97, no. 1, pp. 1–5, 2019.
[50] D. Yousri, S. B. Thanikanti, D. Allam, V. K. Ramachandaramurthy, and M. B. Eteiba, "Fractional chaotic ensemble particle swarm optimizer for identifying the single, double, and three diode photovoltaic models' parameters," *Energy*, vol. 195, Mar. 2020, Art. no. 116979.
[51] L. Wang, K. Sun, Y. Peng, and S. He, "Chaos and complexity in a fractional-order higher-dimensional multicavity chaotic map," *Chaos, Solitons Fractals*, vol. 131, Feb. 2020, Art. no. 109488.
[52] Y. Peng, K. Sun, D. Peng, and W. Ai, "Dynamics of a higher dimensional fractional-order chaotic map," *Phys. A, Stat. Mech. Appl.*, vol. 525, pp. 96–107, Jul. 2019.
[53] D. Yousri, T. S. Babu, D. Allam, V. K. Ramachandaramurthy, E. Beshr, and M. B. Eteiba, "Fractional chaos maps with flower pollination algorithm for partial shading mitigation of photovoltaic systems," *Energies*, vol. 12, no. 18, p. 3548, Sep. 2019.
[54] P. Sharma and T. S. Bhatti, "Performance investigation of isolated wind–diesel hybrid power systems with WECS having PMIG," *IEEE Trans. Ind. Electron.*, vol. 60, no. 4, pp. 1630–1637, Apr. 2011.
[55] A. M. Kassem and A. Y. Abdelaziz, "Reactive power control for voltage stability of standalone hybrid wind–diesel power system based on functional model predictive control," *IET Renew. Power Gener.*, vol. 8, no. 8, pp. 887–899, Nov. 2014.
[56] A. H. Gandomi, X.-S. Yang, S. Talatahari, and A. H. Alavi, "Firefly algorithm with chaos," *Commun. Nonlinear Sci. Numer. Simul.*, vol. 18, no. 1, pp. 89–98, Jan. 2013.
[57] G.-C. Wu, D. Baleanu, and S.-D. Zeng, "Discrete chaos in fractional sine and standard maps," *Phys. Lett. A*, vol. 378, nos. 5–6, pp. 484–487, Jan. 2014.
[58] E. Rashedi, H. Nezamabadi-pour, and S. Saryazdi, "GSA: A gravitational search algorithm," *Inf. Sci.*, vol. 179, no. 13, pp. 2232–2248, Jun. 2009.
[59] X.-S. Yang, "Firefly algorithm, stochastic test functions and design optimisation," 2010, *arXiv:1003.1409*. [Online]. Available: http://arxiv.org/abs/1003.1409
[60] S. Mirjalili, S. M. Mirjalili, and A. Lewis, "Grey wolf optimizer," *Adv. Eng. Softw.*, vol. 69, pp. 46–61, Mar. 2014.
[61] S. Das, Swagatam, A. Biswas, S. Dasgupta, and A. Abraham, "Bacterial foraging optimization algorithm: Theoretical foundations, analysis, and applications," in *Foundations of Computational Intelligence*, vol. 3. Berlin, Germany: Springer, 2009, pp. 23–55.

[62] X. Yang and A. Hossein Gandomi, "Bat algorithm: A novel approach for global engineering optimization," *Eng. Computations*, vol. 29, no. 5, pp. 464–483, Jul. 2012.
[63] X. S. Yang, "Flower pollination algorithm for global optimization," in *Proc. Int. Conf. Unconv. Comput. Nat. Comput.* Berlin, Germany: Springer, Sep. 2012, pp. 240–249.
[64] S. Mirjalili, "Dragonfly algorithm: A new meta-heuristic optimization technique for solving single-objective, discrete, and multi-objective problems," *Neural Comput. Appl.*, vol. 27, no. 4, pp. 1053–1073, May 2016.
[65] J. Derrac, S. García, D. Molina, and F. Herrera, "A practical tutorial on the use of nonparametric statistical tests as a methodology for comparing evolutionary and swarm intelligence algorithms," *Swarm Evol. Comput.*, vol. 1, no. 1, pp. 3–18, Mar. 2011.

YASHAR MOUSAVI (Student Member, IEEE) was born in Shiraz, Iran. He received the B.Sc. degree in electronics engineering from NaghsheJahan University, Isfahan, Iran, and the M.Sc. degree in control engineering from the Shahrood University of Technology, Shahrood, Iran, in 2011 and 2014, respectively. He is currently pursuing the Ph.D. degree with the Department of Applied Science, School of Computing, Engineering and Built Environment, Glasgow Caledonian University, Glasgow, U.K.

His research interests include evolutionary optimization, renewable energy, robotics, robust nonlinear control, fractional-order control, and fault-tolerant control.

ALIREZA ALFI (Senior Member, IEEE) received the B.S. degree from the Ferdowsi University of Mashhad, Mashhad, Iran, in 2000, and the M.S. and Ph.D. degrees from the Iran University of Science and Technology, Tehran, Iran, in 2002 and 2007, respectively, all in electrical engineering.

He joined the Shahrood University of Technology, Shahrood, Iran, in 2008, where he is currently a Full Professor of electrical engineering. His research interests include control theory, fractional order control, time delay systems, and optimization.

IBRAHIM BEKLAN KUCUKDEMIRAL (Senior Member, IEEE) received the B.Sc., M.Sc., and Ph.D. degrees in electrical engineering from Yildiz Technical University, Istanbul, in 1997, 1999, and 2002, respectively.

Between 1998 and 2004, he held the Research and Teaching Assistant position at the Division of Control Systems, Department of Electrical Engineering. From 2004 to 2010, he served as an Assistant Professor and was awarded an Associate Professorship by the Turkish Higher Education Council, in 2010. From 2010 to 2015, he served as an Associate Professor for the Department of Control and Automation Engineering, where he conducted research as a Full Professor, between 2015 and 2017. He is currently a Lecturer in control engineering with the School of Computing, Engineering and Built Environment, Glasgow Caledonian University, Glasgow, U.K. His general research interest includes the broad domain of robust and optimal control systems. His particular research interests include linear matrix inequality-based analysis and synthesis techniques for uncertain time-delayed systems. He is a Member of IFAC and a Fellow of the Higher Education Academy.